THRESHOLD MODELS FOR RAINFALL AND CONVECTION: DETERMINISTIC VERSUS STOCHASTIC TRIGGERS *

SCOTT HOTTOVY†, SAMUEL N. STECHMANN†‡

Abstract. This paper investigates stochastic models whose dynamics switch depending on the state/regime of the system. Such models have been called "hybrid switching diffusions" and exhibit "sliding dynamics" with noise. Here the aim is an application to models of rainfall, convection, and water vapor, where two states/regimes are considered: precipitation and non-precipitation. Regime changes are modeled with a "trigger function," and four trigger models are considered: deterministic triggers (i.e. Heaviside function) or stochastic triggers (finite-state Markov jump process), with either a single threshold for regime transitions or two distinct thresholds (allowing for hysteresis). These triggers are idealizations of those used in convective parameterizations of global climate models, and they are investigated here in a model for a single atmospheric column. Two types of results are presented here. First, exact statistics are presented for all four models, and a comparison indicates how the trigger choice influences rainfall statistics. For example, it is shown that the average rainfall is identical for all four triggers, whereas extreme rainfall events are more likely with the stochastic trigger. Second, the stochastic triggers are shown to converge to the deterministic triggers in the limit of fast transition rates. The convergence is shown using formal asymptotics on the Master-Fokker-Planck equations, where the limit is an interesting Fokker-Planck system with Dirac delta coupling terms. Furthermore, the convergence is proved in the mean-square sense for pathwise solutions.

Key words. Moist atmospheric convection, Sliding Dynamics, Hybrid Switching Diffusions, Convective Parameterization

AMS subject classifications. 00A69, 60J70, 86A10

1. Introduction.

This paper is related to stochastic models that exhibit sliding dynamics with noise [29, 28] and hybrid switching diffusions [36]. In particular here, these types of stochastic models arise in the context of an atmospheric science problem: What is the best way to model the onset and demise of atmospheric convection and/or rainfall?

The mathematical form of the model is

$$dq = S_\sigma \, dt + D_\sigma \, dW, \tag{1.1}$$

where $q \in \mathbb{R}$ is a scalar. The drift S_σ and diffusion D_σ coefficients are constant and have a form that switches when the discrete process σ_t switches its value. For simplicity, σ_t will be a two-state process that takes the value 0 or 1. Furthermore, the dynamics of σ_t will take one of two forms. In one case, the value of σ_t switches when q_t reaches a fixed threshold (which will be labeled q^c or q^{np}),–i.e., $\sigma_t = \mathcal{H}(q_t - q^c)$. We refer to this type of trigger as a "deterministic trigger." This is similar to the sliding dynamics with noise discussed in [29, 28], except here the diffusion D_σ is state-dependent, and two thresholds, q^c and q^{np}, are used in a way that allows hysteresis. In the second case, σ_t is a Markov jump process whose transition rates depend on q_t. Specifically, the transition rates have a form that *allows* a transition to occur when q_t crosses the fixed threshold q^c, but the transition occurs stochastically at some random value of $q > q^c$. We call this a "stochastic trigger." The two different types of triggers with one or two thresholds gives four different models. We call the models with a stochastic trigger with one or two thresholds S1 and S2, respectively. Similarly, the models with a deterministic trigger are referred to as D1 and D2. See Figure 1.1

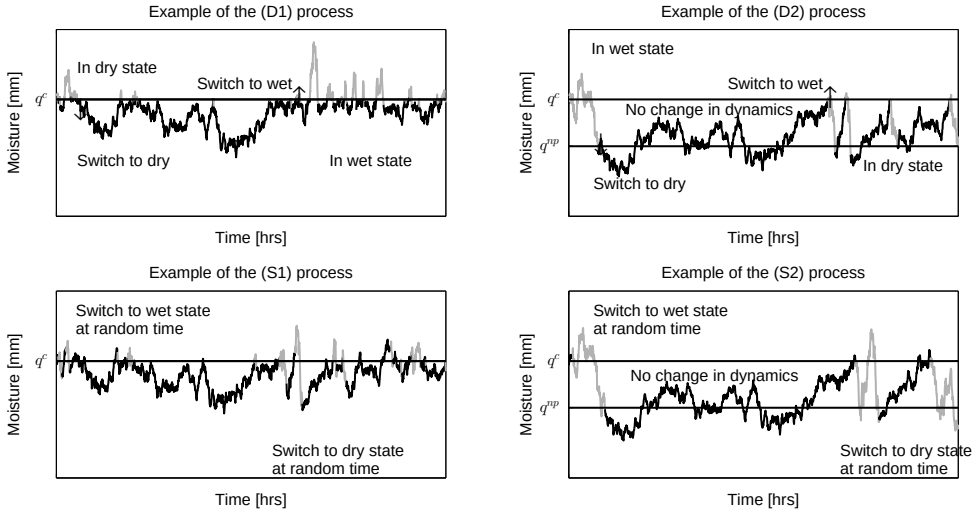

FIG. 1.1. *An example of the four different models used in this study. For all models, the switch to the wet state (grey line) occurs when the threshold q^c is reached from below. For the 1 threshold models (left), the switch to the dry state (black line) occurs when the threshold q^c is reached from above. For the 2 threshold models (right), on the other hand, the switch to dry state occurs when a different threshold q^{np} is reached from above. These switches occur deterministically (top, D) or stochastically (bottom, S). For the deterministic trigger models (top panels), the switch from one state to the other occurs immediately when the threshold is reached. For the stochastic trigger models (bottom panels), on the other hand, the switch from one state to the other does not occur immediately when the threshold is reached; instead, there is a stochastic delay in the switching, and the switching occurs at a random value of q beyond the threshold.*

for sample trajectories of each model. In this way, the "stochastic trigger" σ_t process should converge to the "deterministic trigger" σ_t process as the transition rate λ tends to infinity. One of the main objectives of this paper is to investigate this convergence and to explore the statistics of q_t and σ_t in each of the two cases.

From an atmospheric science point of view, these are idealized stochastic models for rainfall. The variable q_t represents the amount of water vapor in an atmospheric column, which extends vertically above an area of roughly 10 km $\times$ 10 km—perhaps even 100 km $\times$ 100 km. Within such an atmospheric column, clouds and rainfall will occasionally develop, and the development can occur so rapidly that it appears to be "triggered." To describe the trigger mathematically, one simple approach is to use an indicator function σ_t that equals 1 when the column is raining and 0 when there is no rain.

The problem of modeling the trigger σ_t is important for both general circulation models [2, 16, 33] and for hydrological models of rainfall [3, 10, 26, 5, 27, 1]. The D1 model is an idealization of parameterizations of convection in general circulations models and idealized atmospheric models [2, 22, 17, 8, 30]. In the models considered here, two thresholds (q^c and q^{np}) will be used [32] instead of the single threshold q^c,

†Department of Mathematics, University of Wisconsin–Madison
‡Department of Atmospheric and Oceanic Sciences, University of Wisconsin–Madison
*The research of S.N.S. is partially supported by the ONR Young Investigator Program through grant ONR N00014- 12-1-074, and S.H. is supported as a postdoctoral research associate on this grant.

and the two cases will be compared and contrasted. The motivation for introducing a second threshold q^{np} comes from Figure 6 of [21]; this figure shows that more than half of all rainfall occurs below q^c; hence it may be most realistic to use a second threshold q^{np} for the shutdown of rainfall. Stochastic trigger models with smoothed versions of Heaviside functions have been studied previously [18, 19, 31]. This alternative is perhaps more realistic than the use of a Heaviside function, since there is likely no unique, fixed threshold value q^c that demarcates the transition from raining to non-raining for every rain event; nevertheless, the simplicity of the Heaviside function is appealing.

The motivation for the present investigation is threefold.

First, in general circulation models of the atmosphere, the trigger is a key element of the convective parameterization, and it can have significant effects on the realism of tropical convection, convectively coupled waves, and the Madden–Julian Oscillation [16, 14]. While "deterministic triggers" are traditionally used [2, 22, 17, 8, 30], "stochastic triggers" have been proposed and advanced to improve the simulated variability of tropical convection and waves [18, 13, 19, 12, 7]. The models of the present paper can be thought of as idealized versions of realistic stochastic triggers. As such, their value is that they offer exactly solvable statistics for ease of comparison of the two types of triggers; and they allow for proofs of convergence with the rate of convergence with respect to the transition rate. This also provides mathematically rigorous guidance for how the two types of triggers are different.

Second, this paper provides a better understanding of models for a new perspective on precipitation and water vapor observations [24, 21, 23]. The observed statistics have shown a similarity with critical phenomena and other statistical physics paradigms. To better understand the physical processes underlying these statistics, Stechmann and Neelin [31] designed and analyzed a model of the form (1.1), and they showed that the model reproduces many of the observed statistics. Subsequently, Stechmann and Neelin [32] introduced a simpler version of the model that uses deterministic triggers instead of stochastic triggers. The model with deterministic triggers is advantageous because its exact statistics are easily accessible; however, this simplification comes at the expense of slightly less realistic statistics. Hence, for future studies, an important question is: how closely related are the models with deterministic and stochastic triggers? Can the approximation error be quantified? Also along these lines, exact statistics are presented here for a case with stochastic triggers; this case involves a simpler parameter regime than in [31], and some of the formulas can be prohibitively complex compared to the deterministic-trigger model of [32].

Third, the model is an example of hybrid switching diffusions and random dynamical systems with sliding dynamics not studied before. The models, S1 and S2, are examples of switching diffusion systems with discontinuous transition functions defined in equation (2.2), which differs from the examples in [36]. The D1 and D2 models are examples of dynamical systems that undergo sliding dynamics with state–dependent noise. Furthermore, the D2 model has a manifold $q^{np} \leq q \leq q^c$ where the dynamics of the system depend on the state of σ_t. That is, the state of σ_t can not be derived from the moisture value of $q^{np} \leq q_t \leq q^c$ alone.

In this paper, we prove that the hybrid switching diffusion model S2 converges to deterministic trigger model D2 as the transition rate tends to infinity. To do so, we use the Fokker-Planck equation to derive the first and second moments of the jumping time, i.e. the time it takes the λ–process to jump once it reaches the critical threshold. The first and second moments are of order $\lambda^{-1/2}$ which ultimately controls

the L^2 convergence.

The models here are mathematically tractable idealizations of the atmosphere, and they neglect or simplify many aspects of atmospheric physics and dynamics. A more complete description would require other variables besides just water vapor (e.g., temperature) and would require knowledge of the water vapor $q(z,t)$ at each height z above the Earth's surface $z=0$, rather than just the column-averaged water vapor q_t that is considered here. Also, a more complete description would partition rainfall into stratiform and deep convective components [12, 7, 11, 20]. Despite the simplicity of the models here, they contain the important ingredients of thresholds and stochastic forcing which are mainstays in both complex and idealized models alike.

The outline of the paper is as follows: In § 2, we give a more detailed explanation of the models S1,S2,D1, and D2. In § 3 we study numerous properties of the model. First we derive the Fokker–Planck equation for D2 using an asymptotic expansion of the S2 Fokker-Planck equation [§ 3.2]. Then we find the exact stationary solutions for the four models [§ 3.3], and use them to study conditional and marginal statistics [§ 3.4]. We compare the mean event sizes for S2 and D2 in § 3.5. In § 4, we prove the main theorem of the paper [Theorem 4.1], that the S2 process converges, in L^2, to the D2 process as λ tends to infinity.

2. Model Description. In this section we introduce a simple stochastic equation to model water vapor for a single atmospheric column. The column water vapor at time t, denoted q_t is defined by the stochastic different equation (SDE),

$$dq_t^\lambda = \begin{cases} mdt + D_0 dW_t & \sigma_t^\lambda = 0 \\ -rdt + D_1 dW_t & \sigma_t^\lambda = 1, \end{cases} \tag{2.1}$$

with $m > 0$ for moistening and $r > 0$ for rain rates, $D_1 > D_0 > 0$ are the noise coefficients, and the initial condition $q_0^\lambda = q_0, \sigma_0^\lambda = 0$. The dynamics of $\sigma_t^\lambda \in \{0,1\}$ are as follows: when $\sigma_t^\lambda = 0$ the probability that σ^λ transitions to 1 is governed by an exponential random variable with the transition rate $r_{01}(q_t)$. Similarly, when $\sigma_t^\lambda = 1$ the transition rate is $r_{10}(q_t)$. That is, when $\sigma_t = 0$, the probability that the process transitions to the rain state after a short amount of time, $\sigma_{t+\Delta t} = 1$, is given approximately by $r_{01}(q_t)\Delta t$, and similarly for the transition from 1 to 0. The values $q = q^c$ and $q = q^{np} = q^c - q^\epsilon$, for q^ϵ relatively small compared to q^c, play a critical role in the transition to and from convection.

There are many possible physically realistic choices for the rate function $r_{ij}(q)$. For example, in [31] the rate function is a hyperbolic tangent function. Another choice would be to set $r_{01}(q) = 0$ for $q < q^c$ and $r_{01}(q) = 1$ once $q = q^c$. Thus, the process switches dynamics after an exponential random time. SDE, in which a smooth rate function for the switching process is used, are studied in [36]. In this paper, we use the rate functions

$$\begin{cases} r_{01}(q) = \lambda \mathcal{H}(q - q^c) \\ r_{10}(q) = \lambda \mathcal{H}(q^{np} - q). \end{cases} \tag{2.2}$$

The above rate function is studied in this paper because exact formulas are derived, such as the stationary density [Sec. 3.3] and the jumping time distribution — i.e. when $q_t = q^c$ or q^{np}, the time it takes to switch dynamics.

The solution q_t of SDE (2.1) is a Brownian motion with positive ($\sigma = 0$) or negative ($\sigma = 1$) drift. Once the process switches dynamics, the process is still a Brownian motion with drift. Thus, (q_t, σ_t) is a Markov process, and despite the discontinuity of the coefficients of SDE (2.1) there exists a unique solution (see § 4).

We call the above model, the stochastic model with two thresholds (q^c and q^{np}) or S2. Three other models that are closely related to the above are considered in this paper, S1, D1, and D2. The stochastic model with one threshold (q^c), called S1, is interpreted as the above model with $q^{np} = q^c - q^\epsilon \to q^c$ as $q^\epsilon \to 0$. The transition rates for these two models are diagrammed in Figure 2.1. The two deterministic models, with one threshold and two (D1 and D2) are interpreted in the same way as the stochastic, except that the process σ switches dynamics immediately when hitting the threshold. This can be interpreted as having an infinite transition rate.

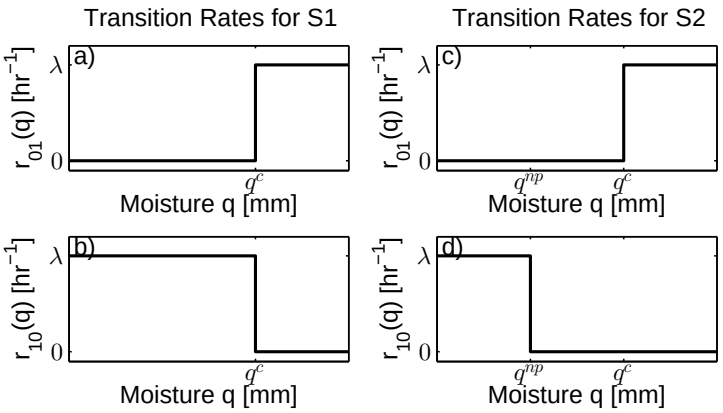

FIG. 2.1. *The transition rates for the S1 and S2 models are shown above. The one threshold model S1 is plotted on the left. The two threshold model S2 is plotted on the right.*

Later in the paper [§ 4], these models are shown to be approximations to one another when a certain limit is taken. I.e. the one threshold models are approximations to the corresponding two threshold models for $q^\epsilon \ll 1$, and the deterministic models are approximations to the stochastic models for $\lambda \gg 1$. The convergence is mapped out in Figure 2.2, and is discussed in Section 4. Note that the jumping time used in this paper is longer than an exponential random time as soon as the threshold is reached and the hyperbolic tangent rate function used in [31]. Thus proving that the above model converges to D2, implies many other models (e.g. the model in [31]) converge as well.

$$\begin{array}{ccc} (\mathrm{S2}) & \xrightarrow{\lambda\to\infty} & (\mathrm{D2}) \\ \Big\downarrow{\scriptstyle q^\epsilon\to 0} & \searrow\!\!\!\!\!\!\Rightarrow{\scriptstyle q^\epsilon\to 0,\ \lambda\to\infty} & \Big\Downarrow{\scriptstyle q^\epsilon\to 0} \\ (\mathrm{S1}) & \overset{\lambda\to\infty}{\Rightarrow} & (\mathrm{D1}) \end{array}$$

FIG. 2.2. *A figure describing the convergence of the separate models. The arrows "$\to$" imply convergence in L^2, and "$\Rightarrow$" are weak convergence (or in distribution), see § 4.*

3. Properties of the Models. In this section, we derive the Fokker-Planck equations for the models D1 and D2. This includes giving a heuristic derivation of the Fokker-Planck equation for D2 [§ 3.2] in the limit as $\lambda \to \infty$. With these equations we solve for exact statistics of the models. The statistics that we study here, for the four different models, are the stationary probability density function [§ 3.3], conditioned statistics computed from the stationary density [§ 3.4], and the event duration [§ 3.5]. These statistics are exactly solvable for the four models.

3.1. The Fokker-Planck Equation for S2. To study the stationary density of the models described in § 2, we use the Fokker-Planck (or Kolmogorov forward) equation for the SDE of the corresponding model. The addition of a continuous time discrete valued process σ_t adds another term to the classic Fokker-Planck equation. For example, consider the process (q_t, σ_t) governed by SDE (2.1) with the S2 type of trigger. Then σ has a q-dependent generator, such that for a suitable function $\phi(q)$,

$$Q(q)\phi(q) = \begin{pmatrix} -\lambda\mathcal{H}(q-q^c) & \lambda\mathcal{H}(q-q^c) \\ \lambda\mathcal{H}(q^{np}-q) & -\lambda\mathcal{H}(q^{np}-q) \end{pmatrix} \begin{pmatrix} \phi_0(q) \\ \phi_1(q) \end{pmatrix}. \tag{3.1}$$

Given the SDE for the process q_t, the joint generator for (q, σ) is

$$\mathcal{L}_{(q,\sigma)} f(q) = \begin{pmatrix} \mathcal{L}_0 f_0(q) & 0 \\ 0 & \mathcal{L}_1 f_1(q) \end{pmatrix} + Q(q) f(q), \tag{3.2}$$

where $\mathcal{L}_i$ is the generator of SDE (2.1) with $\sigma = i$, $i = 0, 1$ [9, 36]. The Fokker-Planck equation is the adjoint of the generator $\mathcal{L}_{(q,\sigma)}$ above. It is a coupled PDE with solutions $\rho_0(q,t), \rho_1(q,t)$. In a slight abuse of terminology, we refer to these solutions as "densities" of the dry (ρ_0) and wet (ρ_1) states, respectively. However, ρ_0 and ρ_1 do not integrate to one. They arise naturally from the joint density, $\rho(q,\sigma,t)$, by partitioning the density into $\sigma = 0$ and $\sigma = 1$, i.e.

$$\rho(q,\sigma,t) = \delta_{\sigma 0}\rho(q,0,t) + \delta_{\sigma 1}\rho(q,1,t) = \rho_0(q,t) + \rho_1(q,t). \tag{3.3}$$

In the case for S2 the Fokker-Planck equation is

$$\begin{aligned} \frac{\partial}{\partial t}\begin{pmatrix} \rho_0(q,t) \\ \rho_1(q,t) \end{pmatrix} = &-\frac{\partial}{\partial q}\begin{pmatrix} m & 0 \\ 0 & -r \end{pmatrix}\begin{pmatrix} \rho_0(q,t) \\ \rho_1(q,t) \end{pmatrix} + \frac{1}{2}\frac{\partial^2}{\partial q^2}\begin{pmatrix} D_0^2 & 0 \\ 0 & D_1^2 \end{pmatrix}\begin{pmatrix} \rho_0(q,t) \\ \rho_1(q,t) \end{pmatrix} \\ &+\lambda\begin{pmatrix} -\mathcal{H}(q-q^c) & \mathcal{H}(q^{np}-q) \\ \mathcal{H}(q-q^c) & -\mathcal{H}(q^{np}-q) \end{pmatrix}\begin{pmatrix} \rho_0(q,t) \\ \rho_1(q,t) \end{pmatrix}. \end{aligned} \tag{3.4}$$

The total probability of the system is conserved, where the state of the system is characterized by the column water vapor $q \in \mathbb{R}$ and the precipitation indicator $\sigma \in \{0, 1\}$. Thus we have the condition

$$\sum_{\sigma=0}^{1} \int_{-\infty}^{\infty} \rho(q,\sigma,t)\, dq = \int_{-\infty}^{\infty} \rho_0(q,t) + \rho_1(q,t)\, dq = 1, \tag{3.5}$$

for all $t \in [0, \infty)$.

The Fokker-Planck equation for S1 can easily be recovered from the formula above by taking $q^{np} = q^c$.

3.2. Derivation of the Limit Fokker-Planck Equation for D2. The Fokker-Planck equation for D2 and D1 will not contain the generator term for stochastic jumps. Instead, it will contain delta function terms which account for the injection of probability mass into the domain of $\sigma = 0$ from $\sigma = 1$ and vice versa. D2 is derived from taking the limit of S2 as $\lambda \to \infty$. The Fokker-Planck equation for D2 was studied in [32], and is

$$\begin{aligned} \tfrac{\partial}{\partial t}\rho_0 &= -m\tfrac{\partial}{\partial q}\rho_0 + \tfrac{D_0^2}{2}\tfrac{\partial^2}{\partial q^2}\rho_0 - \delta(q-q^{np})\, f_1|_{q=q^{np}}\,, & -\infty < q < q^c, t \geq 0, \\ \tfrac{\partial}{\partial t}\rho_1 &= r\tfrac{\partial}{\partial q}\rho_1 + \tfrac{D_1^2}{2}\tfrac{\partial^2}{\partial q^2}\rho_1 + \delta(q-q^c)\, f_0|_{q=q^c}\,, & q^{np} < q < \infty, t \geq 0, \\ \rho_0(q^c,t) &= \rho_1(q^{np},t) = 0 & t \geq 0, \end{aligned} \tag{3.6}$$

where

$$f_0 = m\rho_0 - \frac{D_0^2}{2}\frac{\partial}{\partial q}\rho_0, \tag{3.7}$$

$$f_1 = -r\rho_1 - \frac{D_1^2}{2}\frac{\partial}{\partial q}\rho_1. \tag{3.8}$$

The delta functions in the PDE above can also be viewed as interface conditions on the flux (probability current). It is not clear from equation (3.4) that delta terms will arise. In [32] this system was presented intuitively, and here we derive it from S2 using asymptotics.

To derive the Fokker-Planck equation (3.6) from equation (3.4) we consider the region $q > q^c$. The following analysis will be identical for the region $q < q^{np}$. We first change variables to $\xi = \lambda^{1/2}(q - q^c)$, or $q = \lambda^{-1/2}\xi + q^c$. PDE (3.4) in this region, with the change in variables for the ρ_0 equation only, is

$$\frac{\partial}{\partial t}\rho_0 = -\lambda^{1/2} m\partial_\xi \rho_0 + \lambda\frac{D_0^2}{2}\frac{\partial^2}{\partial \xi^2}\rho_0 - \lambda H(\lambda^{-1/2}\xi)\rho_0 \tag{3.9}$$

We expand the solutions in an asymptotic expansion, only this time, in powers of $\lambda^{-1/2}$. That is,

$$\rho_0 = \rho_0^{(0)}(\xi,t) + \lambda^{-1/2}\rho_0^{(1)}(\xi,t) + \lambda^{-1}\rho_0^{(2)}(\xi,t) + ... \tag{3.10}$$

This results in the system,

$$O(\lambda) \qquad 0 = \frac{D_0^2}{2}\frac{\partial^2}{\partial \xi^2}\rho_0^{(0)} - \rho_0^{(0)} \tag{3.11}$$

$$O(\lambda^{1/2}) \qquad 0 = -m\frac{\partial}{\partial \xi}\rho_0^{(0)} + \frac{D_0^2}{2}\frac{\partial^2}{\partial \xi^2}\rho_0^{(1)} - \rho_0^{(1)} \tag{3.12}$$

$$O(1) \qquad \frac{\partial}{\partial t}\rho_0^{(0)} = -m\frac{\partial}{\partial \xi}\rho_0^{(1)} + \frac{D_0^2}{2}\frac{\partial^2}{\partial \xi^2}\rho_0^{(2)} - \rho_0^{(2)} \tag{3.13}$$

Now we show the following: (i) $\rho_0^{(0)} = 0$ and hence is $\rho_0|_{q^c} = 0$ an absorbing boundary condition. (ii) We solve for the coefficient of the $\rho_0^{(1)}$ term ($C_3(t)$) in the limit as $\lambda \to \infty$. (iii) The Dirac-delta coupling term is derived.

To show $\rho_0^{(0)} = 0$, we give the solution to the $O(\lambda)$ equation [Eq. (3.11)],

$$\rho_0^{(0)}(\xi,t) = C_1(t)\exp\left(-\frac{\sqrt{2}}{D_0}\xi\right) + C_2(t)\exp\left(\frac{\sqrt{2}}{D_0}\xi\right). \tag{3.14}$$

The solution $\rho_0^{(0)}$ is assumed to be a density and hence integrable on (q^c, ∞), thus $C_2(t) = 0$. Furthermore we assume $\rho_0(q,t)$ and $\frac{\partial}{\partial q}\rho_0(q,t)$ are continuous on $\mathbb{R}$ and the limit as $\lambda \to \infty$ must exist everywhere. Note that,

$$\lim_{\lambda\to\infty} \frac{\partial}{\partial q}\rho_0(q,t)|_{q=q^c} = \lim_{\lambda\to\infty} -C_1(t)\lambda^{1/2}\frac{\sqrt{2}}{D_0} + \frac{\partial}{\partial \xi}\rho_0^{(1)}(\xi,t)\bigg|_{\xi=0} + ... \tag{3.15}$$

which does not exist. Thus $C_1(t) = 0$ and $\rho_0^{(0)} = 0$. The solution to the order $\lambda^{1/2}$ equation [Eq. (3.12)] with the integrability condition is

$$\rho_0^{(1)} = C_3(t)\exp\left(-\frac{\sqrt{2}}{D_0}\xi\right). \tag{3.16}$$

By continuity of the probability density,

$$\rho_0((q^c)^-, t) = \lambda^{-1/2}\rho_0^{(1)}(0^+, t) + ... \tag{3.17}$$

Because the right hand side of the above equation decays in λ then for the limit as $\lambda \to \infty$, $\rho_0(q^c, t) \to 0$ for all $t \geq 0$, which implies the absorbing boundary condition for PDE (3.6). By continuity of the derivative at q^c,

$$\frac{\partial}{\partial q}\rho_0((q^c)^-, t) = \frac{\partial}{\partial \xi}\rho_0^{(1)}(0^+, t) + \lambda^{-1}\rho_0^{(2)}(0^+, t) + ... \tag{3.18}$$

$$= -C_3(t)\frac{\sqrt{2}}{D_0} + ... \tag{3.19}$$

In the limit as $\lambda \to \infty$, the above equation, when multiplied by the appropriate constant, is a balance of fluxes at q^c. Therefore,

$$C_3(t) = \frac{\sqrt{2}}{D_0} f_0\bigg|_{q^c}, \tag{3.20}$$

where the flux f_0 is defined as

$$f_0(q,t) = -m\rho_0(q,t) - \frac{D_0^2}{2}\frac{\partial}{\partial q}\rho_0(q,t). \tag{3.21}$$

Next we show the $\lambda\rho_0 \approx \lambda^{1/2}\rho_0^{(1)}$ term converges to a delta function in the sense of distributions. Let $\phi(q)$ be a test function on $\mathbb{R}$. Recall the definition of ξ, thus we have

$$\int_0^\infty C_3(t)\exp\left(-\frac{\sqrt{2}}{D_0}\xi\right)\phi(\xi\lambda^{-1/2} + q^c)\, d\xi \tag{3.22}$$

$$= \int_{q^c}^\infty \lambda^{1/2} C_3(t)\exp\left(-\lambda^{1/2}\frac{\sqrt{2}}{D_0}(q - q^c)\right)\phi(q)\, dq.$$

Integration by parts yields,

$$\int_{q^c}^\infty \lambda^{1/2} C_3(t)\exp\left(-\lambda^{1/2}\frac{\sqrt{2}}{D_0}(q - q^c)\right)\phi(q)\, dq = -\phi(q^c)\frac{D_0}{\sqrt{2}}C_3(t) \tag{3.23}$$

$$+ \int_{q^c}^\infty C_3(t)\frac{D_0}{\sqrt{2}}\phi'(q)\exp\left(-\lambda^{-1/2}\frac{D_0}{\sqrt{2}}(q - q^c)\right)\, dq$$

$$\to C_3(t)\frac{D_0}{\sqrt{2}}\phi(q^c), \tag{3.24}$$

as $\lambda \to \infty$. Thus, using equation (3.20) for $C_3(t)$,

$$\lambda \mathcal{H}(q - q^c)\rho_0 \approx \lambda^{1/2}\rho_0^{(1)} \to \delta(q - q^c) f_0|_{q=q^c}\,, \quad \text{as } \lambda \to \infty. \tag{3.25}$$

Along with a similar argument for the interval $-\infty \le q \le q^{np}$, we recover equation (3.6) in a limit of equation (3.4) as $\lambda \to \infty$.

3.2.1. Deriving the D1 Fokker-Planck equation from D2. Given equation (3.6) for D2, we derive the Fokker-Planck equation for D1. To do so, we take $q^{np} = q^c - q^\epsilon$ and take the limit as $q^\epsilon \to 0$. The non-trivial part of this limit lies with the interface conditions imposed by the delta functions. That is, if we integrate each equation over their respective domains, we get the single condition,

$$f_0(q^c) = f_1(q^{np}). \tag{3.26}$$

Because of the absorbing boundary conditions, equation (3.26) is written in terms of ρ_0 and ρ_1 as

$$\frac{D_0^2}{2}\frac{\partial}{\partial q}\rho_0(q^c) = \frac{D_1^2}{2}\frac{\partial}{\partial q}\rho_1(q^{np}). \tag{3.27}$$

In the limit as $q^\epsilon \to 0$, the above equation is a condition that must be satisfied. Thus, the Fokker-Planck equation for D1 is

$$\begin{cases} \frac{\partial}{\partial t}\rho_0 &= -m\frac{\partial}{\partial q}\rho_0 + \frac{D_0^2}{2}\frac{\partial^2}{\partial q^2}\rho_0, & q < q^c \\ \frac{\partial}{\partial t}\rho_1 &= r\frac{\partial}{\partial q}\rho_1 + \frac{D_1^2}{2}\frac{\partial^2}{\partial q^2}\rho_1, & q > q^c \\ \frac{D_0^2}{2}\frac{\partial}{\partial q}\rho_0(q^c) &= \frac{D_1^2}{2}\frac{\partial}{\partial q}\rho_1(q^c) & \\ 1 &= \int_{-\infty}^{\infty}\rho_0(q,t) + \rho_1(q,t)\,dq & \end{cases} \tag{3.28}$$

The above system does not require $\rho = \rho_0 + \rho_1$ to be continuous. In fact, for $D_0 \neq D_1$, ρ is discontinuous at $q = q^c$. This is seen in the stationary density of D1 [Eq. (3.39)].

3.3. Stationary Density. In this section we compute the stationary densities for the four models using the stationary Fokker-Planck equations. We begin by finding the stationary densities for the S2 model, denoted $\rho_0^\lambda(q)$, $\rho_1^\lambda(q)$ respectively. For S2 the stationary Fokker-Planck equation is

$$\begin{pmatrix}0\\0\end{pmatrix} = -\frac{\partial}{\partial q}\begin{pmatrix} m & 0 \\ 0 & -r\end{pmatrix}\begin{pmatrix}\rho_0^\lambda(q)\\ \rho_1^\lambda(q)\end{pmatrix} + \frac{1}{2}\frac{\partial^2}{\partial q^2}\begin{pmatrix} D_0^2 & 0 \\ 0 & D_1^2\end{pmatrix}\begin{pmatrix}\rho_0^\lambda(q)\\ \rho_1^\lambda(q)\end{pmatrix} \tag{3.29}$$

$$+\lambda\begin{pmatrix} -\mathcal{H}(q-q^c) & \mathcal{H}(q^{np}-q) \\ \mathcal{H}(q-q^c) & -\mathcal{H}(q^{np}-q)\end{pmatrix}\begin{pmatrix}\rho_0^\lambda(q)\\ \rho_1^\lambda(q)\end{pmatrix}. \tag{3.30}$$

The above equation is solved by considering the solution on the intervals $(-\infty, q^{np}], [q^{np}, q^c], [q^c, \infty)$ separately, then using continuity of ρ_0, ρ_1 and their derivatives.

For the stationary density of S2 define,

$$r^\lambda = \frac{-r + \sqrt{r^2 + 2D_1^2\lambda}}{D_1^2}, \quad \text{and} \quad m^\lambda = \frac{m - \sqrt{m^2 + 2D_0^2\lambda}}{D_0^2}. \tag{3.31}$$

The stationary density on the different intervals is,

$$\rho_1(q) = \frac{2rm}{(m+r)\left(q^\epsilon + \frac{m^\lambda - r^\lambda}{r^\lambda m^\lambda}\right)(2r + D_1^2 r^\lambda)} e^{r^\lambda (q - q^{np})}, \qquad q < q^{np}, \tag{3.32}$$

$$\rho_1(q) = \frac{m\left\{1 - e^{-\frac{2r(q-q^{np})}{D_1^2}}\right\}}{(r+m)\left(q^\epsilon + \frac{m^\lambda - r^\lambda}{r^\lambda m^\lambda}\right)} + \frac{r^2 m e^{\frac{2r(q-q^{np})}{D_1^2}}}{\lambda(m+r)\left(q^\epsilon + \frac{m^\lambda - r^\lambda}{r^\lambda m^\lambda}\right) D_1^2}, \qquad q^{np} \le q \le q^c, \tag{3.33}$$

$$\rho_1(q) = \frac{rme^{m^\lambda (q - q^c)}}{(m+r)(2r + D_1^2 m^\lambda)\left(q^\epsilon + \frac{m^\lambda - r^\lambda}{r^\lambda m^\lambda}\right)} \tag{3.34}$$

$$+ \frac{m\left[\frac{r^\lambda D_1}{2r + D_1 r^\lambda} - \frac{m^\lambda D_1}{2r + D_1 m^\lambda} e^{-\frac{2rb}{D_1^2}}\right] e^{-\frac{2r(q-q^c)}{D_1^2}}}{(m+r)\left(q^\epsilon + \frac{m^\lambda - r^\lambda}{r^\lambda m^\lambda}\right)}, \qquad q \ge q^c,$$

and the stationary density for ρ_0 is expressed by a similar formula.

The stationary density for S1 is found by taking the above formula, substituting $q^{np} = q^c - q^\epsilon$ and taking the limit as $q^\epsilon \to 0$. The resulting density is

$$\rho_1(q) = \frac{2mrm^\lambda r^\lambda}{(m+r)(m^\lambda - r^\lambda)(2r + D_1^2 r^\lambda)} e^{r^\lambda (q - q^c)}, \qquad \text{for } q < q^c, \tag{3.35}$$

$$\rho_1(q) = \frac{2mrm^\lambda r^\lambda}{(m+r)(2r + D_1^2 m^\lambda)(m^\lambda - r^\lambda)} e^{r^\lambda (q - q^c)} \tag{3.36}$$

$$+ \frac{2mrm^\lambda r^\lambda D_1^2}{(m+r)(2r + D_1^2 m,^\lambda)(2r + D_1^2 r^\lambda)} e^{-\frac{2r}{D_1^2}(q - q^c)}, \qquad \text{for } q > q^c,$$

and similarly for ρ_0.

The stationary densities for D2, $\rho_0(q), \rho_1(q)$, were given analytically in [32] as

$$\rho_1(q) = \frac{1}{q^\epsilon} \frac{m}{r+m} \left\{1 - \exp\left(-\frac{2r}{D_1^2}(q - q^{np})\right)\right\}, \qquad \text{for } q^{np} \le q \le q^c, \tag{3.37}$$

$$\rho_1(q) = \frac{1}{q^\epsilon} \frac{m}{r+m} \left[1 - \exp\left(\frac{2r}{D_1^2} q^\epsilon\right)\right] \exp\left(-\frac{2r}{D_1^2}(q - q^c)\right), \qquad \text{for } q > q^c, \tag{3.38}$$

and similarly for ρ_0.

The stationary density for D1 by taking $q^\epsilon \to 0$, results in

$$\rho_0(q) = \frac{2rm}{D_0^2(r+m)} \exp\left(\frac{2m}{D_0^2}(q - q^c)\right), \qquad \text{for } q < q^c, \tag{3.39}$$

$$\rho_1(q) = \frac{2rm}{D_1^2(r+m)} \exp\left(-\frac{2r}{D_1^2}(q - q^c)\right), \qquad \text{for } q > q^c. \tag{3.40}$$

Note that the density $\rho = \rho_0 + \rho_1$ is discontinuous for $D_0 \neq D_1$.

The densities are plotted in Figure 3.1, and they can be compared with observed densities [24, 21]. All four models capture the main observed features such as a peak

density just below the threshold q^c and an exponential tail above the threshold q^c. The D1 and D2 models have a slightly unrealistic lack of smoothness near q^c; however, these model densities are quite similar to the S1 and S2 densities for the value $\lambda^{-1} = 0.4$h, which is roughly the value suggested by [31]. Furthermore, the mathematical simplicity of the D1 and D2 models is advantageous for analytical studies.

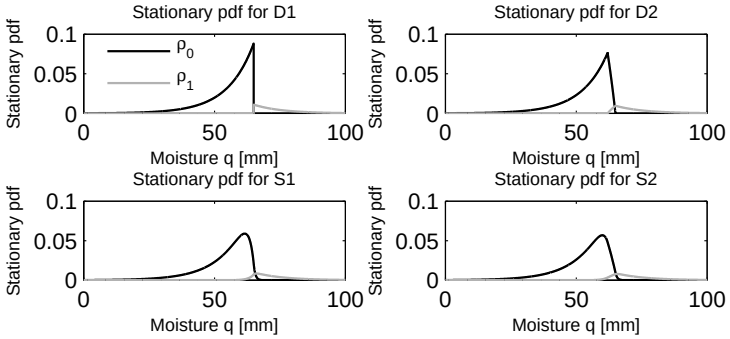

FIG. 3.1. *Plots for the densities of D1, D2 and S1, S2 with $\lambda^{-1} = 0.4h$. The dry state ($\sigma = 0$) is in black and the wet state ($\sigma = 1$) in gray.*

3.4. Conditional and Marginal Statistics. In this section we use the stationary densities calculated above to compute statistics studied in [21]. The stationary densities will be denoted $\rho_0(q), \rho_1(q)$ for the dry and wet states respectively. The same formulas will be used for all four models (S1,S2,D1,D2).

3.4.1. Conditional Mean and Variance of Precipitation. The conditional mean precipitation is defined as the conditional expectation of σ given a moisture value q. That is,

$$E[r\sigma|q] = \frac{r\rho_1(q)}{\rho_0(q) + \rho_1(q)}. \tag{3.41}$$

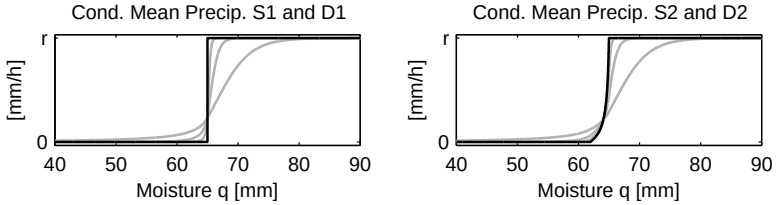

FIG. 3.2. *The mean precipitation is plotted for the deterministic trigger (black lines) and stochastic trigger (gray lines) for $\lambda^{-1} = 4, 0.4, 0.04$ hours with one threshold (left) and two thresholds (right).*

The conditional precipitation variance is defined as the conditional variance of σ given a moisture value q. That is,

$$E[(r\sigma)^2|q] - E[r\sigma|q]^2 = \frac{r^2\rho_1(q)}{\rho_0(q) + \rho_1(q)} - \left(\frac{r\rho_1(q)}{\rho_0(q) + \rho_1(q)}\right)^2. \tag{3.42}$$

The conditional mean precipitation is plotted in Figure 3.2 and the conditional precipitation variance is plotted in the supplemental materials. They can be compared with observed statistics [24, 21]. The two stochastic trigger models (S1,S2) have similar features, such as a smooth pick up near q^c for the mean precipitation and a spike near q^c for the variance, for both one and two thresholds. The D1 model has a Heaviside function for mean precipitation and the variance is zero. When two thresholds are introduced, the D2 model has more realistic features, such as a rapid pick up at q^c for mean precipitation and a spike in the variance. Both of the statistics for S1 and S2 converge to the statistics of D1 and D2 as λ increases.

3.4.2. Average Rainfall. The average rainfall is the fraction of time that the stationary process is in state $\sigma = 1$. It is defined as,

$$E[r\sigma] = \int_{-\infty}^{\infty} r\rho_1(q)\, dq. \tag{3.43}$$

For all four models it is

$$E[r\sigma] = \frac{r^2}{m+r}. \tag{3.44}$$

This means that the average rainfall is invariant in the choice of trigger and threshold. Furthermore, the average rainfall does not change when the transition rate between the dry and wet states are different for stochastic triggers—i.e. when $r_{01} = \lambda H(q-q^c)$ and $r_{10} = \mu H(q^{np} - q)$ with $\mu \neq \lambda$. One explanation is that while the times of the rain events will depend on the choice of trigger (stochastic/deterministic) and thresholds (one or two), these differences will average out in the stationary state. This explanation implies that average rainfall would be preserved under changes to the rate function (i.e. other than a Heaviside function). Further calculations are needed to verify this claim.

The resulting average rainfall variance is

$$E[(r\sigma)^2] - E[r\sigma]^2 = \frac{r^2}{m+r}\left(1 - \frac{r^2}{m+r}\right) = \frac{r^2(m+r-r^2)}{(m+r)^2} \tag{3.45}$$

which is also the same for all four models and independent of λ for S1 and S2.

3.5. Event Size and Event Duration. The event size statistic is defined as the total amount of precipitation to fall, in mm, during a precipitation event. For the models studied here, the event size is proportional to the event duration, which can be solved for exactly.

The event duration probability density for D2 was studied in [32]. The event duration probability density for this case is the first passage probability density for Brownian motion with drift to hit $q^c - q^\epsilon$, the drift and diffusion coefficients are given by SDE (2.1). The event duration density for the wet state, ρ_{1t} is reproduced here,

$$\rho_{1t} = \frac{q^\epsilon}{\sqrt{2\pi D_1^2}} \exp\left\{\frac{rq^\epsilon}{D_1^2}\right\} \exp\left\{\frac{-(q^\epsilon)^2}{2D_1^2 t}\right\} \exp\left\{\frac{-r^2 t}{2D_1^2}\right\} t^{-3/2}, \tag{3.46}$$

and a similar equation holds for ρ_{0t}.

The event duration for S2 is much more complicated. Without loss of generality, let the initial condition $q_0 < q^c$ and $\sigma_0 = 0$. Consider the q^λ process which has just switched dynamics, for the kth time with k odd, from $\sigma = 0$ to $\sigma = 1$, at time t_0. This

is pictured in Figure 3.3. The event time of $\sigma = 1$ is the sum of two random times which we will call τ_k^λ and τ_k^J. The first time, τ_k^λ, is the first passage time from the random point in space $q_{t_0}^\lambda$ where the process switches dynamics to when the process first hits the critical threshold q^{np}. Then the process switches dynamics after a time τ_k^J, which we will call the *jumping time*.

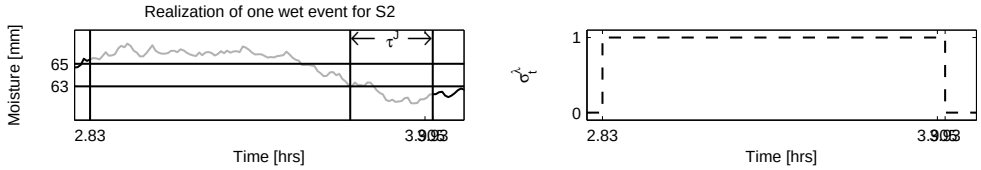

FIG. 3.3. *A realization of the S2 process through one wet event starting at $t = t_0$ and ending when $\sigma_t^\lambda = 1$ for $t > t_0$. The plot on the right is σ_t^λ through the same times.*

3.5.1. Jumping time τ_k^J and position. To study the characteristics of the jumping time τ_k^J for k even (i.e. $\sigma = 0$), we consider the process q^λ with initial condition $q_0^\lambda = q^c$. When the process switches dynamics, we freeze it at the jumping point. Thus we consider the system

$$\begin{cases} \frac{\partial}{\partial t}\rho_0^J(q,t) &= -m\frac{\partial}{\partial q}\rho_0^J(q,t) + \frac{D_0^2}{2}\frac{\partial}{\partial q}^2\rho_0^J(q,t) - \lambda\mathcal{H}(q-q^c)\rho_0^J(q,t) \\ \frac{\partial}{\partial t}\rho_1^J(q,t) &= \lambda\mathcal{H}(q-q^c)\rho_0^J(q,t) \\ \rho_0^J(q,0) &= \delta(q-q^c) \\ \rho_1^J(q,0) &= 0. \end{cases} \tag{3.47}$$

This problem was studied in [25] (see §3.5.3) in the absence of drift. Here we compute the moments of the jumping time for a process with drift. The equation above is solved using Laplace Transforms (see supplementary materials). The exact form of the jumping time density, denoted $\rho_{\tau_k^J}(t)$ is

$$\rho_{\tau_k^J}(t) = \frac{d}{dt}\mathcal{L}^{-1}\left\{\frac{2}{(m+\sqrt{m^2+2D_0^2 s})(-m+\sqrt{m^2+2D_0^2(\lambda+s)})}\right\}, \tag{3.48}$$

where $\mathcal{L}^{-1}$ is the inverse Laplace transform. The mean and second moment are

$$E[\tau_k^J] = \frac{D_0^2}{m}\frac{1}{(-m+\sqrt{m^2+2D_0^2\lambda})}, \tag{3.49}$$

and

$$E[(\tau_k^J)^2] = \frac{D_0^4(2D_0^2\lambda - m(-3m+\sqrt{m^2+2\lambda D_0^2}))}{m^3\sqrt{m^2+2\lambda D_0^2}(m-\sqrt{m^2+2D_0^2\lambda})^2}. \tag{3.50}$$

The corresponding equations for k odd ($\sigma = 1$) are similar. Note that the second moment is order $\lambda^{-1/2}$. This fact is important for the convergence proof in § 4.

Furthermore, we recover an analytic expression for the density of the jumping position. That is, the density for the random position where the process q^λ switched

dynamics. By integrating the equation for ρ_1, in equation (3.47), in time, we see that

$$\lim_{t\to\infty} \rho_1^J(q,t) = \lambda\mathcal{H}(q-q^c)\int_0^\infty \rho_0^J(q,t)\,dt = \lambda\mathcal{H}(q-q^c)\mathcal{L}\{\rho_0^J\}(s=0) \tag{3.51}$$

$$= \frac{2\lambda\mathcal{H}(q-q^c)}{D_0^2(m+\sqrt{m^2+2D_0^2\lambda})} e^{\frac{m-\sqrt{m^2+2D_0^2\lambda}}{D_0^2}(q-q^c)}, \tag{3.52}$$

and similarly for $\sigma = 1$. This density is plotted in Figure 3.4 for various values of λ. The densities all have exponential decay away from q^c and approaches $\delta(q-q^c)$ as $\lambda \to \infty$. This gives the S1 and S2 models the property of delayed onset and demise of convection. Thus the event duration will be longer, on average, than the models of D1 and D2 respectively.

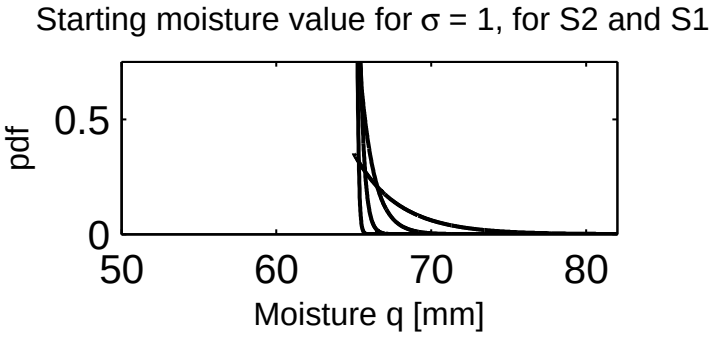

FIG. 3.4. *The density of where the processes S1 and S2 start their rain events for* $\lambda^{-1} = 4, 0.4, 0.04, 0.004h$. *Note that as* λ *increases, the densities are converging to delta functions at* q^c.

3.5.2. First passage time τ_k^λ. Given the distribution of points where the process begins the event, we can calculate the pdf of the first passage time τ_k^λ. The first and second moments of τ_k^λ are found using the Laplace transform (see supplementary materials) and are

$$E[\tau_k^\lambda] = \frac{q^\epsilon}{m} + \frac{D_0^2}{(-r+\sqrt{r^2+2D_1^2\lambda})} \tag{3.53}$$

and

$$E[(\tau_k^\lambda)^2] = \frac{4D_1^4\lambda^2}{(r_+^\lambda)^3(-r_-^\lambda)}\left[\frac{D_0^2 q^\epsilon}{m^3} + \frac{(q^\epsilon)^2}{m^2}\right] \tag{3.54}$$

$$+\frac{D_1^2}{m^3(r_+^\lambda)^3(-r_-^\lambda)}\left(\lambda(2D_1^4 m + 2rq^\epsilon(r_+^\lambda)(D_0^2 - q^\epsilon m) + D_1^2(D_0^2(r_+^\lambda) + 2q^\epsilon(r_+^\lambda)m))\right)$$

where

$$r_\pm^\lambda = \frac{-r \pm \sqrt{r^2+2D_1^2\lambda}}{D_1^2}, \tag{3.55}$$

for k even ($\sigma = 0$) and similarly for k odd.

3.6. Mean and second moment of event size. The mean event size for the q^λ process is

$$E[\tau_k^\lambda + \tau_k^J] = \frac{q^\epsilon}{m} + \frac{D_0^2}{(-r + \sqrt{r^2 + 2D_1^2\lambda})} + \frac{D_0^2}{m}\frac{1}{(-m + \sqrt{m^2 + 2D_0^2\lambda})}. \tag{3.56}$$

and similarly for the $\sigma = 1$ case. The above equation is the sum of the mean event time of the D2 process (q^ϵ/m) and order $\lambda^{-1/2}$ terms.

Because of the Markov property of $(q_t^\lambda, \sigma_t^\lambda)$ the times τ_k^λ and τ_k^J are independent. Therefore, the second moment of the event size is

$$E[(\tau_k^\lambda)^2 + 2\tau_k^\lambda\tau_k^J + (\tau_k^J)^2] = E[\tau_k^2] + 2E[\tau_k^\lambda]E[\tau_k^J] + E[(\tau_k^J)^2]. \tag{3.57}$$

Again, this is the sum of the second moment of the event time of the D2 process and an order $\lambda^{-1/2}$ term.

4. Convergence Theorem. In this section we rigorously prove that the S2 model solution converges to the D2 model solution as $\lambda \to \infty$ in L^2 of the underlying probability space.

THEOREM 4.1. *Let $(q_t^\lambda, \sigma_t^\lambda)$ be the solution of SDE (4.2) with initial conditions (q_0, σ_0) constant for every λ and let (q_t, σ_t) be the solution to SDE (4.3) with the same initial condition (q_0, σ_0). Then*

$$\lim_{\lambda\to\infty} E\left[\sup_{0\le t\le T} |q_t^\lambda - q_t|^2\right] = 0. \tag{4.1}$$

The other modes of convergence pictured in Figure 2.2 are not proved rigorously in this paper, but can be proved either using the strategy of the proof below, or by using well established methods from weak convergence. The proof of Theorem 4.1 takes a path-wise strategy and will highlight where error (between D2 and S2) is introduced in the model, and the decay rate of this error in λ.

In § 4.1 we define the probability space as well as random times where the processes switch dynamics. In § 4.2 we argue that there exists a strong unique solution to the SDE (2.1) for $\lambda < \infty$ and the limiting process D2. In § 4.3 we prove the theorem of L^2 convergence of S2 to D2. In § 4.4 we outline how to prove the other modes of convergence pictured in Figure 2.2. Some estimates and proofs of lemmas used in the proof of Theorem 4.1 are provided explicitly in the supplementary materials.

4.1. Definitions and Notation. Define the joint Markov process $(q_t^\lambda, \sigma_t^\lambda)$ for S2 by the SDE,

$$dq_t^\lambda = \begin{cases} m\,dt + D_0\,dW_t & \text{for } \sigma_t^\lambda = 0 \\ -r\,dt + D_1\,dW_t & \text{for } \sigma_t^\lambda = 1, \end{cases} \tag{4.2}$$

where $\sigma_t^\lambda \in \{0, 1\}$ is a continuous time process defined by the generator in equation (3.1). Define the joint Markov Process (q_t, σ_t) for D2 by the SDE:

$$dq_t = \begin{cases} m\,dt + D_0\,dW_t & \text{for } \sigma_t = 0 \\ -r\,dt + D_1\,dW_t & \text{for } \sigma_t = 1. \end{cases} \tag{4.3}$$

and $\sigma_t \in \{0, 1\}$ is defined in the following manner: If $\sigma_0 = 0$, then the process switches to one at the time when $q_{t_1} = q^{np}$ (i.e. $\sigma_{t_1} = 1$). The process will switch

back to zero at the time when $q_{t_2} = q^{np}$ ($\sigma_{t_2} = 0$), and the algorithm is repeated. For the remainder of this paper, with out loss of generality, we have initial conditions $q_0^\lambda = q_0 < q^c$ and $\sigma_0^\lambda = \sigma_0 = 0$. Note that equations (4.2) and (4.3) differ only in σ_t^λ vs σ_t.

The processes $(q_t^\lambda, \sigma_t^\lambda)$ and (q_t, σ_t) are defined on the same probability space and driven by the same standard Wiener process W_t. The probability space is constructed from two separate spaces. One, we call $(\Omega_1, \mathcal{F}_1, P_1)$ which defines the Wiener process W_t. The other probability triple, $(\Omega_2, \mathcal{F}_2, P_2)$, which is independent of $(\Omega_1, \mathcal{F}_1, P_1)$, defines the exponential random variables which provide the stochastic jumping times of σ_t^λ. The joint probability space is then $(\Omega, \mathcal{F}, P) = (\Omega_1 \times \Omega_2, \mathcal{F}_1 \times \mathcal{F}_2, P_1 \times P_2)$.

Define the stopping times $\mathcal{T}_n, \mathcal{T}_n^\lambda$ as the times where σ_t and σ_t^λ switch values. That is, given the initial condition $q_0 < q^c$, $\sigma_0 = 0$,

$$\mathcal{T}_1 = \inf\{t > 0 : \sigma_t = 1\}, \quad \mathcal{T}_2 = \inf\{t > \mathcal{T}_1 : \sigma_t = 0\}, \quad \mathcal{T}_3 = \inf\{t > \mathcal{T}_2 : \sigma_t = 1\}, ... \tag{4.4}$$

or

$$\mathcal{T}_k = \inf\{t > \mathcal{T}_{k-1} : \sigma_t = \sigma^k\}, \tag{4.5}$$

where $\mathcal{T}_0 = 0$ and

$$\sigma^k = \begin{cases} 0 & \text{for } k \text{ even} \\ 1 & \text{for } k \text{ odd.} \end{cases} \tag{4.6}$$

We similarly define $\mathcal{T}_n^\lambda$ for the process q^λ.

The first passage stopping time, denoted $\tau(x, \hat{q})$, is defined as

$$\tau(x, \hat{q}) = \inf\{s > 0 : q_s = x + \hat{q},\ q_0 = \hat{q}\}, \tag{4.7}$$

and similarly

$$\tau^\lambda(x, \hat{q}) = \inf\{s > 0 : q_s^\lambda = x + \hat{q},\ q_0^\lambda = \hat{q}\}. \tag{4.8}$$

Recall the jumping time τ_k^J, from § 3.5.1, is the time it takes the q^λ process to jump dynamics once it has reached a threshold. I.e., let

$$\hat{t}_k = \inf\{s > \mathcal{T}_{k-1}^\lambda : q_s^\lambda = q^k\}, \tag{4.9}$$

be the time at which the q^λ process reaches one of the thresholds

$$q^k = \begin{cases} q^{np}, & \text{for } k \text{ even} \\ q^c, & \text{for } k \text{ odd.} \end{cases} \tag{4.10}$$

We define the stopping time

$$\tau_k^J = \inf\{s > \hat{t}_k : \sigma_s^\lambda = \sigma^k\}. \tag{4.11}$$

The values of q_t and q_t^λ at those times are shown in the table below [Table 4.1].

The process σ_t is related to a renewal process. Note that we can write

$$\mathcal{T}_k = \begin{cases} 0 & k = 0, \\ \tau(q^c - q_0, q_0) & k = 1, \\ \tau(q^c - q_0, q_0) + \sum_{j=1}^k \tau((-1)^j q^\epsilon, q^j), & k = 2, 3, ... \end{cases} \tag{4.12}$$

Thus the times $\mathcal{T}_i$ have independent increments, and we can define the renewal process N_t

$$N_t = \sum_{i=1}^{\infty} \chi_{\{\mathcal{T}_i < t\}}, \tag{4.13}$$

where χ_A is the indicator function of the set A. Note that N_t is the number of times that σ_t jumps in the interval $[0, t]$.

4.2. Existence and Uniqueness. Both the SDE (4.2) and (4.3), have coefficients which are discontinuous. Thus, the standard existence and uniqueness theorems, which require Lipschitz coefficients, are not applicable here. However, a strong solution exists and is unique. That is, we will show that q_t^λ is a strong solution adapted to the filtration $\mathcal{F}_t = (\mathcal{F}_1)_t \times \mathcal{F}_2$ where $(\mathcal{F}_1)_t = \sigma(W_s, s \le t)$, the smallest sigma algebra generated by the Wiener process. Consider q_t^λ for $0 \le t \le \mathcal{T}_1^\lambda$. Note that $\mathcal{T}_1^\lambda$ is $(\mathcal{F}_1)_t$ measurable. Thus

$$q_t^\lambda = q_0 + mt + D_0 W_t, \quad 0 \le t \le \mathcal{T}_1^\lambda, \tag{4.14}$$

exists and is unique. For $\mathcal{T}_1^\lambda \le t \le \mathcal{T}_2^\lambda$, we define,

$$q_t^\lambda = q_{\mathcal{T}_1^\lambda} - rt + D_0 W_t, \quad \mathcal{T}_1^\lambda \le t \le \mathcal{T}_2^\lambda. \tag{4.15}$$

Therefore, q_t^λ is defined up to $\mathcal{T}_2^\lambda$. This process is repeated up to time T. This method is repeated for the process q_t to show existence and uniqueness for SDE (4.3).

4.3. Proof of Theorem 4.1. *Proof.* To prove the above theorem we must relate individual paths of the processes q^λ and q. An outline of the proof is as follows: first we condition the expectation on the number of jumps N_T that the process σ_t has taken in the interval $[0, T]$. Next, we restrict our processes to a certain ordering of the stopping times $\mathcal{T}_k$ and $\mathcal{T}_k^\lambda$. With this ordering, we consider the difference of the processes at time t. We decompose the difference $|q_t^\lambda - q_t|$ into a finite sum of three types of errors [§ 4.3.1]. These types of errors are estimated to be of order $\lambda^{-1/2}$ (see the supplementary materials for complete estimates). In § 4.3.2 the expectations over the complement of the ordering is shown to be arbitrarily small [Lemma 4.2]. Finally, the probability that $N_T = N$ is shown to decay fast enough so the sums converge [Lemma 4.3]. The estimates on the conditional expectations prove convergence in L^2 with respect to the uniform norm.

To prove Theorem 4.1 we condition on the number of transitions defined by the renewal process N_T [Eq. (4.13)]. Note that $\sup_{0\le t\le T} |q_t^\lambda - q_t|^2$ is a process with parameter T. By the law of total probability,

$$E\left[\sup_{0\le t\le T} |q_t^\lambda - q_t|^2\right] = \sum_{N=0}^{\infty} E\left[\sup_{0\le t\le T} |q_t^\lambda - q_t|^2 \middle| N_T = N\right] P(N_T = N). \tag{4.16}$$

For each finite N the dynamics of q^λ and q can be far out of sync if, for example, $\mathcal{T}_4 < \mathcal{T}_2^\lambda$. In other words, the process q has switched dynamics at least four times where the q^λ process has only switched dynamics twice. Define

$$\mathbb{T}_N = \{\mathcal{T}_1 \le \mathcal{T}_1^\lambda \le \mathcal{T}_2 \le \mathcal{T}_2^\lambda \le \ldots \le \mathcal{T}_{N-1}^\lambda \le \mathcal{T}_N\}. \tag{4.17}$$

Now we break up each conditional expectation into the $\mathbb{T}_N$ and $\mathbb{T}_N^c$ parts. Define,

$$E_{\mathbb{T}_N}[A] = E[A; \mathbb{T}_N] = \int_{\omega\in\mathbb{T}_N} A \, dP(\omega), \tag{4.18}$$

and

$$E_{\mathbb{T}_N^c}[A] = E[A; \mathbb{T}_N^c]. \tag{4.19}$$

We can write

$$\begin{aligned} E\left[\sup_{0\le t\le T}|q_t^\lambda - q_t|^2 \middle| N_T = N\right] =& E_{\mathbb{T}_N}\left[\sup_{0\le t\le T}|q_t^\lambda - q_t|^2 \middle| N_T = N\right] \\ &+ E_{\mathbb{T}_N^c}\left[\sup_{0\le t\le T}|q_t^\lambda - q_t|^2 \middle| N_T = N\right]. \end{aligned} \tag{4.20}$$

We first consider the expectation on the sets $\mathbb{T}_N$, then we will show the probability of $\mathbb{T}_N^c$ is small [§ 4.3.2].

4.3.1. Three different types of errors. We first consider the expectation on $\mathbb{T}_N$ and condition on $N_T = N$. The error will be split into three terms. That is, given the ordering $\mathbb{T}_N$,

$$q_t^\lambda - q_t = \sum_{k=1}^{N_t}\xi_k + \sum_{k=1}^{N_t-1}\zeta_k + \mathcal{E}_t. \tag{4.21}$$

The first type, ξ_k is due to the lag in the jumping time to switch dynamics. We define this error as,

$$\begin{aligned} \xi_k =& (-1)^{k-1}\left(\int_{\mathcal{T}_k^\lambda-\tau_k^J}^{\mathcal{T}_k^\lambda}(m+r)\,ds + \int_{\mathcal{T}_k^\lambda-\tau_k^J}^{\mathcal{T}_k^\lambda}(D_0-D_1)\,dW_s\right) \\ =& (-1)^{k+1}(m+r)\tau_k^J + (-1)^{k-1}(D_0-D_1)\left(W_{\mathcal{T}_k^\lambda} - W_{\mathcal{T}_k^\lambda-\tau_k^J}\right). \end{aligned} \tag{4.22}$$

The second error, which is compounding, accrues when q_t hits a threshold, switches dynamics, then q_t^λ must reach the threshold. We define this as

$$\begin{aligned} \zeta_k =& (-1)^k\tau^\lambda\left((-1)^k\left(\sum_{j=1}^k\xi_j + \sum_{j=1}^{k-1}\zeta_j\right), q^{k+1} + (-1)^{k-1}\left(\sum_{j=1}^k\xi_j + \sum_{j=1}^{k-1}\zeta_j\right)\right)(m+r) \\ &+(-1)^k(D_0-D_1)\left(W_{\mathcal{T}_k+\tau^\lambda\left((-1)^k\left(\sum_{j=1}^k\xi_j+\sum_{j=1}^{k-1}\zeta_j\right), q^{k+1}+(-1)^{k-1}\left(\sum_{j=1}^k\xi_j+\sum_{j=1}^{k-1}\zeta_j\right)\right)}\right. \\ &\left.-W_{\mathcal{T}_k}\right), \end{aligned} \tag{4.23}$$

where $q^k = q^c$ for k odd and q^{np} for k even. The third error, is the last term where the process ends

$$\mathcal{E}_t = (-1)^{N_t-1}\left(\int_{\mathcal{T}_{N_t}}^t(m+r)\,ds + \int_{\mathcal{T}_{N_t}}^t(D_0-D_1)\,dW_s\right). \tag{4.24}$$

Note that this term, in some cases, will be zero (i.e. if $\mathcal{T}_N^\lambda < T$).

To highlight the role of the stopping times and errors, a table of the various stopping times and their ordering is given in Table 4.1. The stopping times are ordered with respect to $\mathbb{T}_N$. The error between the models at $\mathcal{T}_1^\lambda$ (where the λ

Stopping Times τ	q_τ	σ_τ	q_τ^λ	σ_τ^λ
0	q_0	$\sigma_0 = 0$	q_0^λ	$\sigma_0^\lambda = 0$
$\mathcal{T}_1$	q^c	1	q^c	0
$\mathcal{T}_1^\lambda = \mathcal{T}_1 + \tau_1^J$	–	1	–	1
$\mathcal{T}_2$	q^{np}	0	–	1
$\mathcal{T}_2 + \tau^\lambda(-\xi_1, q^{np} + \xi_1)$	–	0	q^{np}	1
$\mathcal{T}_2^\lambda = \mathcal{T}_2 + \tau^\lambda(-\xi_1, q^{np} + \xi_1) + \tau_2^J$	–	0	–	0
$\mathcal{T}_3$	q^c	1	–	0
$\mathcal{T}_3 + \tau^\lambda(\xi_1 + \zeta_1 + \xi_2, q^c - (\xi_1 + \zeta_1 + \xi_2))$	–	1	q^c	0
$\mathcal{T}_3^\lambda$	–	1	–	1
$\vdots$	$\vdots$	$\vdots$	$\vdots$	$\vdots$

TABLE 4.1

A table of the stopping times defined in Section 4.1. The places with a "–" denote random values. Note that we have assumed the ordering $\mathbb{T}_N$.

process jumps), denoted ξ_1, remains constant until the q_t process reaches q^{np}. This is where the second type of error accrues, ζ_1, until the λ process reaches q^{np}.

We provide some explicit examples of ζ_k for clarity.

$$\zeta_1 = -(m+r)\tau^\lambda(-\xi_1, q^{np} + \xi_1) - (D_0 - D_1)(W_{\mathcal{T}_1 + \tau^\lambda(-\xi_1, q^{np}+\xi_1)} - W_{\mathcal{T}_1}) \tag{4.25}$$

$$\begin{aligned}\zeta_2 =&(m+r)\tau^\lambda(\xi_1 + \zeta_1 + \xi_2, q^c - (\xi_1 + \zeta_1 + \xi_2)) \\ &+(D_0 - D_1)(W_{\mathcal{T}_2 + \tau_2^\lambda(\xi_1+\zeta_1+\xi_2, q^c - (\xi_1+\zeta_1+\xi_2))} - W_{\mathcal{T}_2}).\end{aligned} \tag{4.26}$$

Now we square equation (4.21) and using the Cauchy-Schwartz inequality we have

$$|q_t^\lambda - q_t|^2 \le 9N_t^2 \sum_{k=1}^{N_t} \xi_k^2 + 9(N_t - 1)^2 \sum_{k=1}^{N_t - 1} \zeta_k^2 + 9\mathcal{E}_t^2. \tag{4.27}$$

The $\sup_{0\le t\le T} N_t = N_T$. Thus the supremum over $0 \le t \le T$ of both sides of the above equation is

$$\sup_{0\le t\le T} |q_t^\lambda - q_t|^2 \le 9N_T^2 \sum_{k=1}^{N_T} \xi_k^2 + 9(N_T - 1)^2 \sum_{k=1}^{N_T - 1} \zeta_k^2 + 9 \sup_{0\le t\le T} \mathcal{E}_t^2. \tag{4.28}$$

The conditional expectation is

$$\begin{aligned}E_{\mathbb{T}_N}\left[\sup_{0\le t\le T} |q_t^\lambda - q_T|^2 \middle| N_T = N\right] \le& 9N^2 \sum_{k=1}^{N} E_{\mathbb{T}_N}[\xi_k^2] + 9(N-1)^2 \sum_{k=1}^{N-1} E_{\mathbb{T}_N}[\zeta_k^2] \\ &+9E_{\mathbb{T}_N}\left[\sup_{0\le t\le T} \mathcal{E}_t^2\right].\end{aligned} \tag{4.29}$$

We first calculate the expectation of ζ_k. To do so, consider Brownian motion with drift μ and diffusion coefficient D^2, i.e. $\mu\tau + DW_\tau = x$, $W_0 = 0$, and x having the

same sign as μ. The first and second moments of the first passage time, $\tau(x,\hat{q})$, are

$$E[\tau(x,\hat{q})] = \frac{|x|}{|\mu|} \tag{4.30}$$

$$E[\tau(x,\hat{q})^2] = \frac{x^2}{\mu^2} + \frac{D^2|x|}{|\mu|^3} = E[\tau(x,\hat{q})]^2 + \frac{D^2}{|\mu|^3}|x|. \tag{4.31}$$

Using the fact that the expected first passage time is linear in x, an estimate of $E_{\mathbb{T}_N}[\zeta_k^2]$ is,

$$\begin{aligned} E_{\mathbb{T}_N}[\zeta_k^2] \leq & 4(m+r)^2 \frac{1}{c_k^2}\left(E_{\mathbb{T}_N}\left[\left(\sum_{j=1}^{k}\xi_j + \sum_{j=1}^{k-1}\zeta_j\right)\right]\right)^2 \\ & + 4(m+r)^2\frac{D_k^2}{c_k^3}E_{\mathbb{T}_N}\left[\left|\left(\sum_{j=1}^{k}\xi_j + \sum_{j=1}^{k-1}\zeta_j\right)\right|\right] \\ & + 4(D_1-D_0)^2\frac{1}{c_k}E_{\mathbb{T}_N}\left[\left|\left(\sum_{j=1}^{k}\xi_j + \sum_{j=1}^{k-1}\zeta_j\right)\right|\right], \end{aligned} \tag{4.32}$$

where

$$D_k = \begin{cases} D_0, & \text{for } k \text{ even}, \\ D_1, & \text{for } k \text{ odd}. \end{cases} \tag{4.33}$$

Thus the second moment of ζ_k is estimated by the first and second moments of the sums of ξ_j and ζ_j. To prove that the second moment of ζ_k converges to zero as $\lambda \to \infty$ we show that these moments are of order $O(\lambda^{-1/2})$. In order to show ζ_k is $O(\lambda^{-1/2})$ we define the first moment recursively (see the supplementary materials). To prove the theorem, we also bound the second moment of $\mathcal{E}_T$. Combining these estimates of $E[\zeta_k^2]$, $E[\xi_k^2]$, and $E[\mathcal{E}_T^2]$ results in

$$E_{\mathbb{T}_N}\left[|q_t^\lambda - q_t|^2 | N_T = N\right] \leq 4N^2\sum_{i=1}^{N}E[\xi_i^2] + 4(N-1)^2\sum_{i=1}^{N-1}E[\zeta_i^2] + \mathcal{E}_T = O(N^6\lambda^{-1/2}). \tag{4.34}$$

4.3.2. Complement of $\mathbb{T}_N$. Now we show that the expectation over $\mathbb{T}_N^c$ is small. No matter the ordering of the stopping times, the biggest the error can be is if $|\sigma_s - \sigma_s^\lambda| = 1$ for all $s \in [0,t]$. Thus by Doob's maximal inequality,

$$\begin{aligned} E_{\mathbb{T}_N^c}\left[\sup_{0\leq t\leq T}|q_t^\lambda - q_t|^2 \middle| N_T = N\right] \leq & E_{\mathbb{T}_N^c}\left[\sup_{0\leq t\leq T} t^2(r+m)^2 \middle| N_T = N\right] \\ & + E_{\mathbb{T}_N^c}\left[\sup_{0\leq t\leq T}(D_1-D_0)^2|W_t - W_0|^2 | N_T = N\right] \\ \leq & T^2(r+m)^2 E_{\mathbb{T}_N^c}[1|N_T = N] + T(D_1-D_0)^2 E_{\mathbb{T}_N^c}[1|N_T = N] \qquad (4.35) \\ \leq & \left(T^2(r+m)^2 + T(D_1-D_0)^2\right)P(\mathbb{T}_N^c). \qquad (4.36) \end{aligned}$$

Now we show that the probability of $\mathbb{T}_N^c$ converges to zero as $\lambda \to \infty$.

LEMMA 4.2. *Let $T < \infty$, and let N be the finite, random number of times that the process q switches dynamics. For all $\epsilon > 0$, there exists some $\Lambda_N \in \mathbb{R}$ such that for all $\lambda \geq \Lambda_N$,*

$$P(\mathbb{T}_N^c) < \epsilon. \tag{4.37}$$

See the supplementary materials for the proof.

Using inequalities (4.34), and (4.36), for all $\epsilon > 0$ we have

$$\begin{aligned} E\left[\sup_{0\leq t\leq T}|q_t^\lambda - q_t|^2\right] = &\sum_{N=0}^{\infty}\left(E_{\mathcal{T}_N}\left[\sup_{0\leq t\leq T}|q_t^\lambda - q_t|^2\middle| N_T = N\right]\right. \qquad (4.38)\\ &\left. + E_{\mathcal{T}_N^c}\left[\sup_{0\leq t\leq T}|q_t^\lambda - q_t|^2\middle| N_T = N\right]\right)P(N_T = N)\\ \leq &C\sum_{N=0}^{\infty}\left(N^6\lambda^{-1/2} + \epsilon\right)P(N_T = N) \qquad (4.39)\end{aligned}$$

Because N_T is a renewal process with finite mean and second moment,

$$\sum_{N=0}^{\infty}\epsilon P(N_T = N) = C_T\epsilon. \tag{4.40}$$

However the terms in the sum of the right hand size of inequality (4.39) are of order $N^6P(N_T = N)$. We now prove a lemma about the decay properties of $P(N_T = N)$ for large N.

LEMMA 4.3. *Let N_T be the renewal process defined in equation (4.13) at time $T < \infty$. Then there exists some N_0 and constants $a > 0$ and $C > 0$ depending on N_0, such that for all $N > N_0$*

$$P(N_T = N) \leq Ce^{-aN}. \tag{4.41}$$

See the supplemental materials for the proof.

With this lemma, the sum in inequality (4.39) is finite, and

$$\sum_{N=0}^{\infty}N^6\lambda^{-1/2}P(N_T = N) \leq C\lambda^{-1/2}. \tag{4.42}$$

Therefore,

$$\begin{aligned} E\left[\sup_{0\leq t\leq T}|q_t^\lambda - q_t|^2\right] \leq &C\sum_{N=0}^{\infty}\left(N^6\lambda^{-1/2} + \epsilon\right)P(N_T = N) \qquad (4.43)\\ \leq &\tilde{C}(\lambda^{-1/2} + \epsilon), \qquad (4.44)\end{aligned}$$

and $\epsilon > 0$ is arbitrarily small. Therefore

$$\lim_{\lambda\to\infty}E\left[\sup_{0\leq t\leq T}|q_t^\lambda - q_t|^2\right] = 0. \tag{4.45}$$

□

While Theorem 4.1 describes the mean error, one might also investigate fluctuations in the error about the mean. In terms of equation (4.21), the error is a sum of random variables. The first sum, with the ξ_i, are independent and identically distributed random variables with finite mean and second moment. Therefore, a central limit type theorem can be proved for the first sum, and the error grows like N. For the second sum, the random variable ζ_i are not independent or identically distributed. However, the second moment of ζ_k, is finite and it grows like k^2. Thus, if a stronger property of ζ_k can be proven, i.e. Markov or Martingale, then a central limit type theorem will hold for the second sum (see [15] § 2.6).

4.4. Convergence of other models. The other convergence theorems of the models (pictured in Figure 2.2), can be proved using a similar argument as above ($S2 \to S1$) or by weak convergence proofs that are well developed. That is, showing the generators of the process, defined in equation (3.2), converge to the limiting process' generator. For example, the argument in § 3.2 can be made rigorous. For an example and outline of such a proof see [6] Chapter 6, and [4] for a complete treatment.

5. Conclusion. Four models were investigated for the initiation and termination of rainfall events. In the trigger for the events, the models use the water vapor q in an atmospheric column. Two triggers were considered (deterministic vs. stochastic), and two threshold scenarios were considered (a single threshold vs. two distinct thresholds). These cases are motivated by triggers used in or proposed for use in the convective parameterizations of global climate models.

The results presented here were of two types: exact statistics and convergence results. For example, it was shown that the average rainfall was identical for all four triggers. However, with a stochastic trigger, a larger mean and variance for duration of rainfall coupled with a larger initial column water vapor and delayed demise of the rain event imply extreme rainfall events are more likely than with deterministic triggers. Furthermore, the exact statistics were utilized in a rigorous proof of pathwise convergence in a mean-square sense: the stochastic triggers converge to deterministic triggers in the limit of fast transition rates. The proof also shows the error between the stochastic and deterministic trigger as a sum random variables which characterizes the fluctuations about the mean. Besides this rigorous pathwise proof, convergence of the generators was also demonstrated using formal asymptotics. In this latter case, the asymptotic limit is an interesting Fokker-Planck system with Dirac delta coupling terms.

The models presented here are examples of hybrid switching diffusions (stochastic trigger) and random dynamical systems exhibiting sliding dynamics (deterministic trigger). As examples within these classes of dynamics, the models here exhibit several interesting features. With a deterministic trigger, the model is of the class of random dynamical systems with sliding dynamics and state-dependent noise. When one threshold is used the stationary probability density function has a discontinuity at q^c. For two thresholds, the system allows for hysteresis and the paths q_t and q_t^λ are not Markovian. The stochastic trigger model is an example of a hybrid switching diffusion. The models presented here use a transition function $r_{ij}(q)$ which has a jump at q^c or q^{np}.

Generalizations of the present models would be necessary to make them fitting for global climate models. For instance, the full vertical structure would be needed as $q_t(z)$, rather than the column-averaged water vapor q_t. Also, a more complex trigger

could use not only water vapor but also temperature, convective available potential energy (CAPE), convective inhibition (CIN), etc.

The idealized triggers here illustrate two ways to extend existing convective parameterizations. First, distinct thresholds could be used for the initiation and termination of events. Here these were labeled q^c and q^{np}, and they introduced an element of hysteresis. Moreover, they introduce a realistic element of uncertainty; specifically, given an atmospheric state q in the range $q^{np} < q < q^c$, it is uncertain whether it is precipitating or not. Second, a stochastic trigger could be used to delay the onset of precipitation events and allow the build-up of a high humidity environment. Such a delayed onset has sometimes led to improved simulations of tropical convection and the Madden–Julian Oscillation, although it is typically achieved through modifications of the convective entrainment rate [35, 16, 34].

When replacing a deterministic trigger with a stochastic trigger, the single–column results here suggest an improved realism of some detailed event statistics while still maintaining the same value of climatological mean rainfall. Such a result would be desirable for global climate models, since modifying the convective parameterization can sometimes improve convective variability while adversely affecting the climatological mean state, or vice versa.

REFERENCES

[1] P. Bernardara, C. De Michele, and R. Rosso, *A simple model of rain in time: An alternating renewal process of wet and dry states with a fractional (non-Gaussian) rain intensity*, Atmos. Res., 84 (2007), pp. 291–301.

[2] A. K. Betts and M. J. Miller, *A new convective adjustment scheme. Part II: Single column tests using GATE wave, BOMEX, ATEX and arctic airmass data sets*, Q. J. Roy. Met. Soc., 112 (1986), pp. 693–709.

[3] D. R. Cox, *Renewal theory*, Methuen, London, 1962.

[4] S. N. Ethier and T. G. Kurtz, *Markov processes*, Wiley Series in Probability and Mathematical Statistics: Probability and Mathematical Statistics, John Wiley & Sons Inc., New York, 1986. Characterization and convergence.

[5] E. Foufoula-Georgiou and D. P. Lettenmaier, *A markov renewal model for rainfall occurrences*, Water Resour. Res., 23 (1987), pp. 875–884.

[6] J.P. Fouque, J. Garnier, G. Papanicolaou, and K. Sølna, *Wave propagation and time reversal in randomly layered media*, vol. 56 of Stochastic Modelling and Applied Probability, Springer, New York, 2007.

[7] Y. Frenkel, A. J. Majda, and B. Khouider, *Stochastic and deterministic multicloud parameterizations for tropical convection*, Clim. Dyn., 41 (2013), pp. 1527–1551.

[8] D. M. W. Frierson, A. J. Majda, and O. M. Pauluis, *Large scale dynamics of precipitation fronts in the tropical atmosphere: a novel relaxation limit*, Commun. Math. Sci., 2 (2004), pp. 591–626.

[9] C. W. Gardiner, *Handbook of stochastic methods for physics, chemistry and the natural sciences*, vol. 13 of Springer Series in Synergetics, Springer-Verlag, Berlin, third ed., 2004.

[10] J. R. Green, *A model for rainfall occurrence*, J. Roy. Statist. Soc. Ser. B, 26 (1964), pp. 345–353.

[11] R. A. Houze, Jr., *Observed structure of mesoscale convective systems and implications for large-scale heating*, Q. J. Roy. Met. Soc., 115 (1989), pp. 425–461.

[12] B. Khouider, J. A. Biello, and A. J. Majda, *A stochastic multicloud model for tropical convection*, Comm. Math. Sci., 8 (2010), pp. 187–216.

[13] B. Khouider, A. J. Majda, and M. A. Katsoulakis, *Coarse-grained stochastic models for tropical convection and climate*, Proc. Natl. Acad. Sci. USA, 100 (2003), pp. 11941–11946.

[14] B. Khouider, A. J. Majda, and S. N. Stechmann, *Climate science in the tropics: waves, vortices and PDEs*, Nonlinearity, 26 (2013), pp. R1–R68.

[15] T. Komorowski, C. Landim, and S. Olla, *Fluctuations in Markov processes*, vol. 345 of Grundlehren der Mathematischen Wissenschaften [Fundamental Principles of Mathematical Sciences], Springer, Heidelberg, 2012. Time symmetry and martingale approximation.

[16] J.L. Lin, M.I. Lee, D. Kim, I.S. Kang, and D.M.W. Frierson, *The impacts of convective parameterization and moisture triggering on AGCM-simulated convectively coupled equatorial waves*, Journal of Climate, 21 (2008), pp. 883–909.

[17] J.W.B. Lin and J.D. Neelin, *Influence of a stochastic moist convective parameterization on tropical climate variability*, Geophys. Res. Lett., 27 (2000), pp. 3691–3694.

[18] A.J. Majda and B. Khouider, *Stochastic and mesoscopic models for tropical convection*, Proc. Natl. Acad. Sci. USA, 99 (2002), pp. 1123–1128.

[19] A. J. Majda and S. N. Stechmann, *Stochastic models for convective momentum transport*, Proc. Natl. Acad. Sci., 105 (2008), pp. 17614–17619.

[20] M. W. Moncrieff and C. Liu, *Representing convective organization in prediction models by a hybrid strategy*, J. Atmos. Sci., 63 (2006), pp. 3404–3420.

[21] J. D. Neelin, O. Peters, and K. Hales, *The transition to strong convection*, J. Atmos. Sci., 66 (2009), pp. 2367–2384.

[22] J. D. Neelin and N. Zeng, *A quasi-equilibrium tropical circulation model—formulation*, J. Atmos. Sci., 57 (2000), pp. 1741–1766.

[23] O. Peters, A. Deluca, A. Corral, J. D. Neelin, and C. E. Holloway, *Universality of rain event size distributions*, J. Stat. Mech., 2010 (2010), p. P11030.

[24] O. Peters and J. D. Neelin, *Critical phenomena in atmospheric precipitation*, Nature Physics, 2 (2006), pp. 393–396.

[25] S. Redner, *A Guide to First-Passage Processes*, Cambridge University Press, Cambridge, 2001.

[26] J. Roldán and D. A. Woolhiser, *Stochastic daily precipitation models: 1. A comparison of occurrence processes*, Water Resour. Res., 18 (1982), pp. 1451–1459.

[27] F. Schmitt, S. Vannitsem, and A. Barbosa, *Modeling of rainfall time series using two-state renewal processes and multifractals*, J. Geophys. Res., 103 (1998), pp. 23181–23193.

[28] D. J. W. Simpson and R. Kuske, *The positive occupation time of brownian motion with two-valued drift and asymptotic dynamics of sliding motion with noise*, ArXiv e-prints, (2012).

[29] ———, *Stochastically perturbed sliding motion in piecewise-smooth systems*, ArXiv e-prints, (2012).

[30] S. N. Stechmann and A. J. Majda, *The structure of precipitation fronts for finite relaxation time*, Theor. Comp. Fluid Dyn., 20 (2006), pp. 377–404.

[31] S. N. Stechmann and J. D. Neelin, *A stochastic model for the transition to strong convection*, J. Atmos. Sci., (2011), pp. 2955–2970.

[32] ———, *First-passage-time prototypes for precipitation statistics*, Journal of the Atmospheric Sciences, (2014).

[33] E. Suhas and G. J. Zhang, *Evaluation of trigger functions for convective parameterization schemes using observations*, J. Climate, (2014), p. accepted.

[34] K. Thayer-Calder and D.A. Randall, *The role of convective moistening in the Madden-Julian oscillation*, J. Atmos. Sci., 66 (2009), pp. 3297–3312.

[35] T. Tokioka, K. Yamazaki, A. Kitoh, and T. Ose, *The equatorial 30–60 day oscillation and the Arakawa–Schubert penetrative cumulus parameterization*, J. Meteor. Soc. Japan, 66 (1988), pp. 883–901.

[36] G. George Yin and Chao Zhu, *Hybrid switching diffusions*, vol. 63 of Stochastic Modelling and Applied Probability, Springer, New York, 2010. Properties and applications.